12-17-2004

Development and Characterization of Controlled Drug Delivery Using Nanoparticles

Li Chen
University of New Orleans

DEVELOPMENT AND CHARACTERIZATION OF CONTROLLED DRUG DELIVERY USING NANOPARTICLES

A Thesis

Submitted to the Graduate Faculty of the
University of New Orleans
in partial fulfillment of the
requirements for the degree of

Master of Science
in
The Department of Chemistry

by

Li Chen

B.S, Zhengzhou University, China, 1993

December 2004

ACKNOWLEDGEMENTS

Firstly, I would like to express my greatest gratitude to my advisor, Prof. Zeev Rosenzweig, not only for his support and invaluable advice on the research work, but also for his encouragement and patience during the past years.

I would also like to thank Prof. Nitsa Rosenzweig for her help in cell cultures; committee member Prof. Matthew A. Tarr and Prof. Jiye Fang for their advices and discussions on the research work.

I would like to thank everyone in my group for their help and advices. I'll remember the time we spent together.

Lastly, I would like to thank my husband Jiachang Gong, my lovely twin girls Katherine and Melinda, my family for their support and sacrifices.

TABLE OF CONTENTS

LIST OF FIGURES

ABSTRACT

The objective of this project was to develop new controlled drug delivery systems using nanomeric particles and characterize the delivery of drugs into cells in real time by digital fluorescence imaging microscopy techniques. The project is based on the idea that it could be possible to improve efficacy of drug molecules when encapsulated in nanometer-sized particles. Due to their small dimensions the particles could permeate through cells and tissues and even through the blood brain barrier.

The anti-cancer drug Doxorubicin was encapsulated into biodegradable Poly (DL-lactide-co-glycolide) (PLGA) nanoparticles by simple nanoprecipitation method. The small size of these particles (<200nm) could be beneficial to realize passive tumor-targeted drug delivery through enhanced permeability and retention (EPR) effects. These drug-containing particles showed a sustained release profile. Fluorescence images indicated that these particles can be internalized by human breast cancer MCF-7 cells by non-specific endocytosis. The bioactivity of the drugs was also tested against cell culture. The results indicated that DXR-loaded PLGA nanoaprticles could be used to deliver Doxorubicin into breast cancer cells.

As the second approach, a novel silica nanoparticles-based stimuli-responsive drug delivery system has been developed. The feasibility of these unique carriers was demonstrated by coating the dye-loaded silica nanoaprticles with phospholipids membrane. The release was induced by the addition of the antimicrobial peptide cecropin (1-8)-melittin (1-18). The advantage of this system is the capability of adjusting drug release rate by external stimuli.

CHAPTER 1 INTRODUCTION

1.1 Controlled Drug Delivery

From the earliest times, people have found ways to introduce drugs into the body. This process began with the chewing of leaves and roots of medicinal plants. Throughout the history of medicine delivery of drugs to humans has evolved from primitive extracts and inhalants to more reliable dosages forms, such as injections, tablets and capsules. These drug delivery systems are expected to be further optimized to increase drug activity and reduce toxicity. For instance, one of the most common ways of administering drugs to the body is via injection into the bloodstream. The injected material is circulated throughout the body and thus commonly termed systemic delivery. The drawbacks of this delivery method are that the concentration of the injected material is extremely diluted and the material acts on most tissues of the body and may be toxic to some of them. The problem could be solved by controlled drug delivery. In controlled drug delivery systems, the active agent is released in a predesigned manner. Drug delivery systems can influence the performance of a drug by manipulating its concentration, location and duration of exposure.

In the past 30 years, controlled drug delivery technology has represented one of the most rapidly advancing research areas [1-5]. The field is driven by the belief that controlled drug delivery

will contribute significantly to human health. These drug delivery systems offer numerous advantages compared to conventional dosage forms:

- increasing the efficacy of currently used drugs
- providing opportunities for the use of new agents currently precluded from clinical use due to challenges including low drug solubility and systemic toxicity
- reducing harmful side effects
- precise control of dose
- decreasing number of dosages
- improving patient compliance and convenience

1.2 Strategy of Controlled Release

There are three strategies to achieve controlled drug delivery. One method is to prepare drug delivery systems that release drugs over extended duration. Numerous works have been done based on biodegradable polymers [6-9]. In the conventional drug delivery, the drug concentration in the blood rises when drug is taken, then peaks and declines. Since each drug has a plasma level above which it is toxic and below which it is ineffective, the plasma drug concentration in a patient at a particular time depends on compliance with the prescribed routine. In contrast, with controlled release systems, the rate of drug release matches the rate of drug elimination. Therefore, the drug concentration is within the therapeutic range for a longer time. This release pattern is highly beneficial for drugs that are rapidly metabolized and eliminated from the body after administration.

The second approach is to prepare a feedback controlled devices that release the appropriate amount of drug in response to a therapeutic marker. In recent years, several research groups have been developing responsive systems [10-14]. These systems can be classified as external regulated and self-regulated systems. The external controlled devices apply external triggers for pulsed delivery such as: magnetic, ultrasonic, thermal and electric triggers. In the self-regulated system, the release rate is controlled by feedback information. The self-regulated systems utilize several approaches such as pH-sensitive polymers, enzyme substrate reactions and competitive binding, as rate-control mechanisms.

The third strategy is to control drug distribution in the body. The idea is to deliver a drug to the precise location in the body where it will be most effective. There are two basic types of targeting systems: passive and active. Passive targeting systems rely on non-specific interactions such as hydrophobic or electrostatic interactions, and the body physical characteristics. The size of drug carriers has been extensively studied for passive targeting. It was found that particles larger than 5-7 μm in diameter usually become trapped in the lung [15] and particles smaller than 1 μm in diameter rapidly phagocytosed by the Kupffer cells of the liver [16]. When the particle size is reduced below 100 nm, the particles can appear in the bone marrow [17]. It was also demonstrated that drug carriers small than 200 nm can be accumulated efficiently in tumor through enhanced permeability and retention (EPR) effect due to the abnormality of tumor tissue, resulting in the enhanced vascular permeability compared to healthy tissues [18-20]. On the other hand, active targeting systems utilize specific interactions, such as antigen-antibody and ligand-receptor binding, to achieve specific targeting goals. In this approach, the therapeutic index of drugs could be enhanced by keeping drugs away from healthy cells. The types of receptors that have been utilized for this purpose include transferrin receptors (tumor cells) [21], folate

receptors (tumor cells) [22], albumin receptors (cardiac and lung) [23] and growth factors receptors [24].

1.3 Scope of Controlled Drug Delivery Systems

While these fundamental ideas of controlled drug delivery are extremely attractive, achieving controlled drug delivery is not a simple or straightforward task. Currently, the vast majority of the work in this area is focusing on liposomes, micelles, drug conjugates, and particles.

1.3.1 Liposomes and Micelles

Although liposomes were initially developed as models of biological membranes, their potential as a drug delivery system have undergone intensive investigations for over 25 years [25]. Liposomes are formed by the equilibration of natural phospholipids with excess water or aqueous salt solution. They contain one or several (concentric) lipid bilayers, which can solubilize hydrophobic drugs. Alternating aqueous compartments can entrap hydrophilic drugs [26-29]. Liposomes with mean diameter smaller than 100 nm selectively spread in leaky tissues (eg. solid tumors), and exhibit target specificity with negligible adverse effects to normal tissues [30].

There are several advantages of liposomes as drug delivery carriers. Liposomes are able to protect drugs from degradation. They are relatively easy to prepare and prevent accumulation of drugs in normal organs which reduces their toxicity and improves pharmacokinetic effects (reduced

elimination, increased circulation life times). When coupled with antibodies, liposomes serve as a means to confer active targeting [31]. Some issues such as contents retention, circulation lifetime, biodistribution and immunogenicity can be managed by the formulation of the liposomal drug carriers [32-34]. Liposome properties such as size, surface charges, membrane rigidity and phase transitions within the bilayer can be controlled either by selecting appropriate lipid compositions or by changing external conditions such as temperature, acidity or the presence of specific agents [35-39]. Liposomes have been used as carriers for many drugs with low molecular weight, peptides [40-45] and oligonucleotides [46, 47]. However, liposomes also have limitations. One of the problems with liposomes as drug delivery carriers is their lack of stability in biological fluids. Consequently, drug molecules leak to normal tissues and cause undesirable side effects.

Micellar drug carriers are formed from amphiphilic block copolmers composed of hydrophilic and hydrophobic segments. The hydrophobic segments form the inner core of the micelle and are surrounded by an outer shell consisting of the hydrophilic segments. Micelles are commonly of the order of 50 nm [48], which compares with the dimension of viruses, and thus may be able to penetrate the sinusoidal and fenestrated capillaries that have pores approximately 100 nm in size. However, micellar carriers are generally considered to be poor delivery systems because micellar complexes are in dynamic equilibrium with free molecules in solution. They continuously break down and reform, and they are generally unstable on dilution.

1.3.2 Drug conjugates

The basic idea is to develop drug conjugates by chemically modify a drug in order to selectively alter properties such as: biodistribution, pharmacokinetics, solubility and antigenicity.

Thus, drugs have been attached to soluble macromolecules such as proteins, polysaccharides, and polymers via degradable linkages [49, 50]. This process changes the drug's size and other properties, resulting in different pharmacokinetics and biodistribution. One active area is to conjugate antitumor drugs to polymers. For example, doxorubicin, an antitumor agent was coupled to N-(2-hydroxypropyl) methacrylamide copolymers, which resulted in radically altered pharmacokinetics and reduced toxicity. The half-life of the drug in plasma and the drug levels in the tumor were increased while the concentrations in the periphery decreased [51]. Polymers such as polyethylene glycol (PEG), can be attached to drugs to lengthen their lifetime. PEG-asparaginase is used for patients with leukemia [52]. Receptors such as transferrin were also used to conjugate antitumor agents for tumor targeting. Recently, dendrimers emerged as promising drug carriers. Compared with polymers, it is relatively easy for dendrimers to control molecular weight and functional groups. Recent studies showed that dendrimers attenuate the toxicity of approved drugs – methotrexate and 6-mercaptopurine, suggesting that higher dosing might be attainable [53].

1.3.3 Nanoparticle and microparticles

The application of nanoparticles and microparticles as drug delivery systems has received increasing attention. They have been widely applied in the delivery of drugs, genes, and vaccines to specific cells and tissues of interest with potential reduction of toxicity as well as increased therapeutic effects [54, 55]. Compared to liposomes, particles appear to offer an interesting alternative. They possess higher stability in biological fluids and during storage. In addition, they have a larger loading capacity than liposomes.

One of widely studied areas is polymer nanoparticles, either natural or synthetic, as drug carriers. Polymer particles have the ability to deliver a wide range of drugs to varying areas of the body for sustained period of time. The active agent can be released from polymeric systems by diffusion, degradation and swelling, depending on the nature of the polymer. The most common used polymers have been poly (lactic acid) (PLA), poly (glycolic acid) (PGA), poly (Є-caprolactone) (PCL) and the copolymer (PLGA) of PLA and PGA, These polymers are known for their biocompatibility and biodegradability [56]. The degradation rate and accordingly, the drug release rate can be manipulated by varying the polymer composition. Other than these polymers, natural hydrophilic polymers such as chitosan, sodium alginate and gelatin have also been used to prepare drug-loaded nanoparticles. These particles have shown good association with proteins, such as bovine serum albulmin, tetanus toxoid, diptaheria toxoid, insulin and oligonucleotides [57-59].

Porous polymeric particles are also attractive as delivery systems due to their special structures. Langer *et al* developed a new type of inhalation aerosol, which is based on porous microparticles composed of 50:50 PLGA and poly (lactic acid-co-lysine-graft-lysine) [60]. Results revealed that inhalation of large porous insulin particles resulted in elevated systemic levels of insulin and suppressed systemic glucose levels for 96 hours, whereas small nonporous insulin particles had this effect for only 4 hours.

Recently, advances in nanomaterials science and biotechnology facilitated the development of new drug delivery systems. Silica naoparticles are well known for their compatibility in biological system [61]. Their surfaces can be easily modified with different functional groups. These features make silica nanoparticles promising as drug carriers. Prasad *et al* demonstrated the potential of ceramic-based nanoparticles as drug carriers for photodynamic therapy [62]. Several other groups explored the potential of porous silica nanoparticles for controlled drug delivery due to their

attractive features such as large surface area, tunable pore sizes and surface properties [63-66]. Their research demonstrated that silica materials could play a significant role in developing a new generation of controlled drug delivery systems.

1.4 Fluorescence and its Applications in Controlled Drug Delivery

1.4.1 Fluorescence

Fluorescence is the property of some molecules and atoms to absorb light at a particular wavelength and to subsequently emit light of longer wavelength after a brief interval. Fluorescence typically occurs from poly-aromatic hydrocarbons or heterocycles molecules that are called fluorescent dyes or fluorophore. Fluorescence occurs when an excited molecule returns to the electronic ground state from the excited singlet state by the emission of a photon.

Fig. 1.1 describes radiative and nonradiative processes that occur following excitation of a molecule. S_0, S_1, S_2, and S_n represent the singlet state of ground, 1^{st}, 2^{nd}, and n^{th} electronic energy levels, respectively. T_1, T_2 represent the triplet states of 1^{st} and 2^{nd} electronic energy levels. The absorption of photons typically occurs from the lowest vibration level of S_0 to a vibration state of S_1 or S_2. After the light was absorbed by the fluorophore, several processes take place. Nonradiative, fast relaxation brings the molecule down to the lowest excited state S_1 within 10^{-12} s. This process is defined as internal conversion. Fluorescence brings back the molecule to one of the vibronic sublevels of the ground state S_0. The fluorescence lifetime of S_1 is generally in the range of 10^{-8} s. alternatively, collisional quenching may bring the molecule

back to its ground state without photon emission. A third type of process presenting in organic dyes is intersystem crossing to the first excited triplet state T_1. Relaxation from this excited state back to the ground state is defined as phosphorescence. The lifetime of this state is in the order of microseconds to milliseconds. The entire fluorescence process is cyclical. Unless the fluorophore is irreversibly destroyed in the excited state, the same fluorophore can be repeatedly excited and detected.

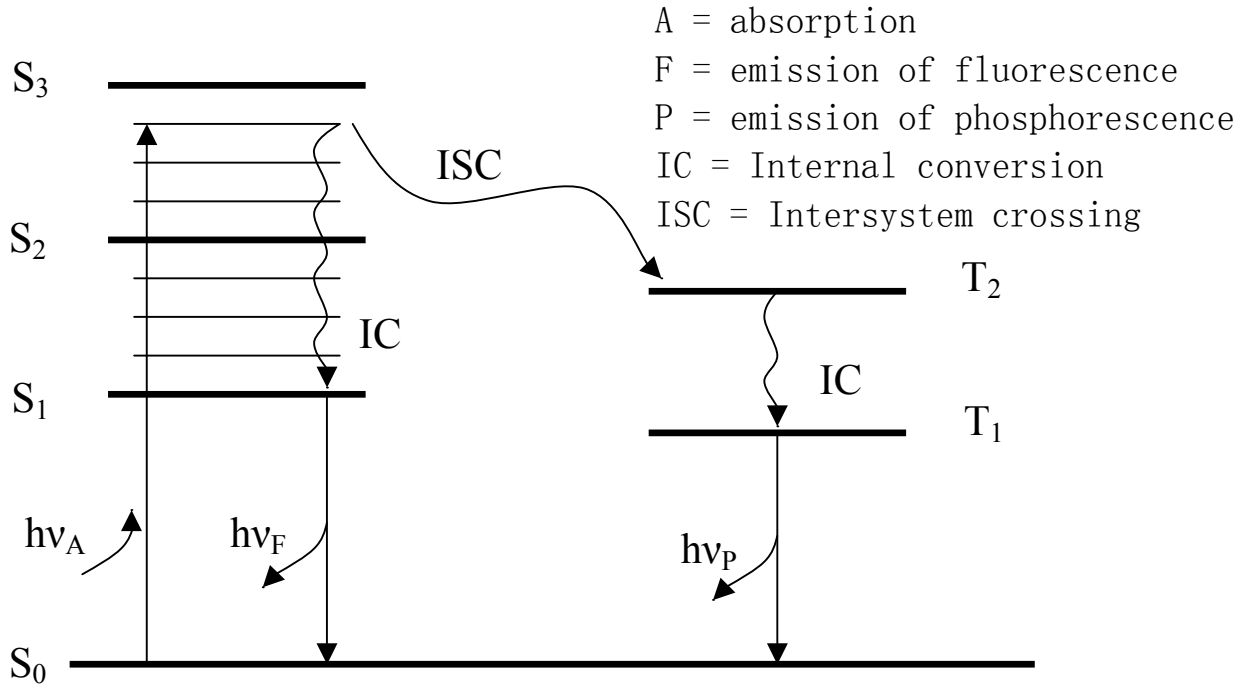

Figure 1.1. Jablonski diagram illustrating the processes involved in the creation of an excited electronic singlet state by optical absorption and subsequent emission of fluorescence and phosphorescence.

1.4.2 Applications in drug delivery

As we mentioned previously, the performance of a drug depends on its location, concentration and duration. Determining the drug biodistribution, cellular fate and cell uptake mechanism would enable better understanding of the cytotoxicity and the drug resistance. Mass spectroscopy is widely used to provide the information about drug delivery into specific organs and tissues. However, it does not offer the information about cellular drug distribution. Imaging techniques are better choices for this purpose. Among them, fluorescence microscopy has been proven to be effective in studying the cellular fate of delivered drugs, due to its high sensitivity and easy-to-use procedure. For example, Savic and his coworkers prepared the tetramethylrhodamine labled PCL-PEO copolymer micelles. A triple-labeling confocal fluorescence microscopy was then developed to identify the location of the micelles [67]. Results revealed that the micelles were located in several cytoplasmic organelles, including mitochondria, but not in the nucleus. They also found that the micelles changed the cellular distribution and increased the amount of agent delivered into the cells.

CHAPTER 2: EXPERIMENTAL

This chapter described the general experimental information and instruments used to carry out the research work. Specific technical and experimental details will be described later in related chapter.

2.1 Materials and Reagents

Poly (DL-lactide-co-glycolide) (PLGA, L/G=50/50, inherent viscosity 0.17dL/g) (Birmingham Polymers, Inc.)

Doxorubicin hydrochloride (Sigma)

Polyvinylalchol (PVA) (average molecular weight 30000-70000 Da, 88% hydrolyzed) (Sigma)

3-(4, 5-dimethyl-2-yl)-2,5-diphenyltetrazolium bromide (MTT) (Molecular Probes)

Tetra ethyl orthosilicate (TEOS) (Sigma)

Hexadecyltrimethylammoniun bromide (CTAB) (Fluka)

Tetramethyl Rhodamine, Dextran 3000 (TMR-Dex)

1,2-Dimyristoyl-sn-Glycero-3-Phosphocholine (DMPC) (Avanti lipids)

1,2-Didocosahexaenoyl-sn-Glycero-3-[Phospho-L-Serine] (Sodium Salt) (PS) (Avanti lipids)

Carboxyl Fluorescein (Sigma)

Cecropin (1-8)-Melittin (1-18) hybrid peptide (CA (1-8)- M (1-18) (Bachem America)

Phosphate Buffered Saline tablet (Amresco)

HEPES (Sigma)

MES (Sigma)

Dullbeco's modified Eagle's medium (invitrogen)

Fetal bovine serum (invitrogen)

Trypsin (invitrogen)

Human breast cancer cell line (MCF-7) (American Type Culture Collection)

Lab-Tek II chambered coverglass (Fisher Scientific)

All aqueous solutions were prepared with 18 MΩ deionized water produced by a water purification system (Barnstead Thermolyne nanopure) and all chemicals were used as received without further purification.

2.2 Procedures and Protocls

2.2.1 Synthesis of PLGA and doxorubicin-loaded nanoaprticles

PLGA particles were prepared using a nanoprecipitation method [68]. Briefly, PLGA was dissolved in acetonitrile with concentrations range from 10 mg/mL to 17 mg/mL. 5 mL PLGA solution were then added dropwisely to a 15 mL PVA solution (1%) under magnetic stirring. The organic solvent was evaporated while being stirred first at atmospheric pressure overnight and then at reduced pressure for 2 hours. The particles were collected by centrifugation for 15 min and washed twice with deionized water to remove PVA residues.

For encapsulation of doxorubicin into nanoparticles, doxorubicin was dissolved in methanol and mixed with the PLGA solution (1:4, V/V), then added to the PVA solution. The procedure was repeated as described above.

2.2.2 Synthesis of mesoporous silica nanoparticles

Mesoporous silica nanoparticles were synthesized based on a method developed by Cai and his coworker [69]. Typically, in a 500 mL flask, 0.5 g hexadecyltrimethyl-ammonium bromide (CTAB) was first dissolved in 240 mL deionized water. Then, 1.75 mL 2 M NaOH solution was added to the CTAB solution. The solution temperature was raised to 353 K while stirring. When the solution became clear, 2.5 mL TEOS was added dropwisely to the surfactant solution. In 2min, the solution became cloudy. The mixture was stirred at about 353K for two

hours. After two hours, the particles were filtered out, washed with DI water and methanol, dried at ambient temperature. To remove the surfactant template, the resulting particles were refluxed in a solution of 160 mL methanol and 15mL 37% hydrochloric acid for 24 hours, filtered a second time and washed with DI water and methanol extensively. Then, the particles were dried with vacuum for 24 hours to remove the trace solvent remained in mesopore.

2.2.3 Drug analog-tetramentylrhodamine dextran loading

To load the drug analog, 70 mg dried mesoprous silica particles were soaked in 1 mL 1 mM TMR-Dex solution at pH 3 for 24 hours. Then, The TMR-Dex loaded silica nanoparticles were isolated by centrifugation at 12000rpm for 5min. The amount of TMR-Dex loaded was determined by monitoring the difference in the fluorescence of solution before and after absorption. Briefly, 10 μL free TMR-Dex solutions were taken from solution before and after absorption, respectively, and then diluted to 1 mL. The difference was calculated using the calibration curve, which was obtained using standard TMR-Dex solution. All measurements were performed in triplicates.

2.2.4 Preparation of drug analog loaded silica with lipids coated (silica lipobeads)

To remove free dye, 250 uL TMR-Dex loaded silica nanoparticles suspensions were washed with pH 3 HCl solution and resuspended in 300 ul pH 5 solutions. To coat the TMR-Dex loaded silica nanoparticles, 1mL 25mM phospolipid chloroform solution were added dropwizely in particles suspensions while strongly vortexing. The resulting emulsion was dried under gentle nitrogen stream firstly to allow the phospholipids molecules absorb onto the surface of particles and then transfer to the vacuum for 6hours to remove organic solvent. Eventually, 5 mL 10 mM HEPES Buffer were added and stirred for 5 hours to form silica lipobeads.

2.2.5 Cell culture

The human breast cancer cell line (MCF-7) was maintained according to protocol provided by ATCC. The cells were cultured at 37^{o}C in a humidified atmosphere with 5% CO_2. They were grown in Dullbeco's modified Eagle's medium (DMEM) supplemented with 10% fetal bovine serum (FBS), 1% Antibiotic-antimycotic, 4% L-glutamine, 1% sodium pyruvate, 1% non-essential amino acids and 0.01 mg/mL insulin. The medium was replaced three times a week.

To prepare subcultures, Cell medium were removed from a cell culture plate and 5 mL trypsin were added. The cells in trypsin solution were incubated for 5-10 minutes and collected. The cell suspensions were centrifuged at 1700 RPM for 10 minutes. After trypsin was removed, the cells were resuspended in fresh cell medium and splited into new plates. Cell cultures on the

surface of a chambered coverglass were also prepared using the above procedure. The MCF-7 cells were detached and placed in a chambered coverglass. Fresh cell medium was then added to chamber and the cells were incubated to attach and grow on the chambered coverglass overnight.

2.3 Instrumentation

2.3.1 Spectrofluorometry

Emission spectra of free dye and dye-loaded naoparticles were obtained using a PTI model QM-1 spectrofluorometer (PTI, Quantmaster, Ontario, Canada). There are three major components in the system: Light source, monochromators and photomutiplier tube (PMT) detector. A 75-W high-pressure xenon (Xe) lamp is used as the excitation light source. Such lamps have a continuous and uniform intensity light output from 250 nm to 700 nm. Two monochromators are employed for selection of excitation and emission wavelength. The monochromators are autocalibrated and under computer control for scanning and positioning. A vacuum PMT with the wavelength range 200-900 nm is employed as the detector. The PMT is a current source with the current being proportional to the light intensity.

2.3.2 Digital fluorescence imaging microscopy

The digital fluorescence imaging microscopy system, which is used for fluorescence measurement of particles and cell experiments are shown in Figure 2.1. The system consists an inverted fluorescence microscopy (Olympus IX-70) equipped with three detection ports. A 100-W mercury lamp is used as the light source. The fluorescence is collected by a 20x or 40x objective with a numerical aperture of 0.50, 0.90 respectively. Filter cube containing a excitation filter, a dichroic mirror and a emission filter was used to obtained the fluorescence images of particles and cells. A slow scan, high performance charged-coupled device (CCD) camera (Andor technology, Model DV 434) with a 1024 × 1024 pixel array is employed to collect digital fluorescence images of the drug containing- particles. A PC-compatible microcomputer is employed for data acquisition using Roper Scientific software winspec 3.2. The image ProPlus software was used for imaging analysis.

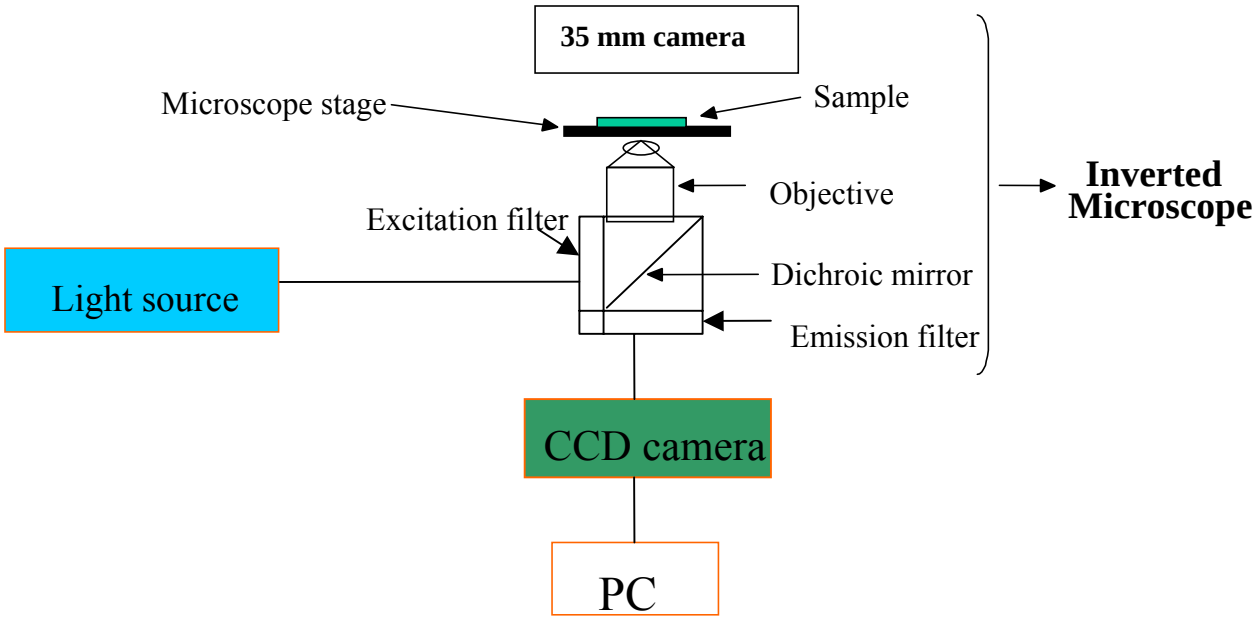

Figure 2.1 Digital Fluorescence Imaging Microscopy System

2.3.3 Transmission Electron Microscopy

The size and morphology of particles were characterized using JEOL EM8291 electron microscopy. The operation voltage is 200 kV.

CHAPTER 3 TUMOR TARGETED DELIVERY OF ANTICANCER DRUG-DOXORUBICIN USING POLYMERIC NANOPARTICLES AS CARRIERS

3.1 Introduction

In the present study, we have entrapped the anti-cancer drug Doxorubicin (DXR) in poly (lactide-co-glycolide) PLGA nanoparticles and evaluated the cytotoxicity on MCF-7 cells. Doxorubicin (DXR) is one of the most widely prescribed antracycline agents. It has been proven to be effective against variety of human malignancies, such as leukemia and breast cancer [70]. The mechanism of action of DXR has been extensively investigated. DXR is a DNA-intercalating agent and a topo-isomerase inhibitor [71]. However, its use is restricted by problems associated with its cardio and systemic toxicity. To improve the therapeutic index of DXR, considerable interests have been drawn to develop submicron carriers-associated DXR formulation such as liposomes [72], micelles [73, 74], and nanoparticles [75-78]. PLGA is the most commonly used biodegradable polymer in drug delivery systems. It was approved by the Food and Drug Administration (FDA) in the United States. Also it's a slow release polymer and often used to sustain a constant level of drug overtime. Yoo et al conjugated DXR with PLGA, then formed nanoparticles and achieved high drug loading. They showed maintained drug activity when comparing drug-conjugate with free drug [78]. In our study, we optimized the

conditions to prepare DXR-loaded PLGA nanoparticles and evaluated the potential of PLGA nanoaprticles as drug carriers for the delivery of doxorubicin into MCF-7 breast cancer cells.

3.2 Specific Experimental and Technical Details

3.2.1 Characterization of nanoparticles

The Shape, surface and size of particles were characterized using Transmission Electron Microscopy (TEM) (JEOL EM8291). Samples were stained with 2% phosphotungstic acid, immobilized on copper grids and dried overnight for viewing. Particle size and size distribution were analyzed by image ProPlus from TEM images taken from different fields.

3.2.2 Fluorescence measurements

Fluorescence spectra of DXR were measured using a PTI international (model QM1) fluorimeter. A 75-W continuous Xe arc Lamp was used as a light source. Emission spectra of DXR were obtained with the excitation wavelength at 480 nm.

3.2.3. Loading studies of DXR

DXR-containing nanoparticles were prepared by the method described in chapter 2. These nanoparticles were washed twice with DI water and collected by centrifugation at 4 ^{o}C. The amount of drug loaded was determined by analyzing the amount of drug present in supernatant. The supernatant concentration was calculated by measuring the emission at 590 nm with excitation wavelength 480 nm. All measurements were performed in triplicates. Encapsulation efficiency was calculated using formula shown below:

% Encapsulation efficiency = (Total DXR- free DXR) /Total DXR

3.2.4 In vitro drug release studies

The *in vitro* release studies of DXR from nanoparticles were carried out in phosphate buffered saline of pH 7.4 and pH 5 buffer solutions at 37^{o}C. 1 mL DXR-containing nanoparticle suspensions were incubated in a water bath at 37 ^{o}C. At various time intervals, the supernatants were isolated by centrifugation for 15 min and their fluorescence spectrum was measured using the fluorimeter. The concentration of doxorubicin in the supernatants was calculated using calibration curves constructed using standard doxorubicin solutions in pH 7.4 and pH 5 buffer solutions. Samples were kept in the dark at all time. All samples were made in triplicates.

3.2.5 In vitro cytotoxic measurements

In vitro cytoxicity against the human breast cancer cell line MCF-7 was determined using tetrazolium dye (MTT) cell proliferation assay [79], which involved the conversion of 3-(4, 5-dimethyl-2-yl)-2, 5-diphenyltetrazolium bromide into an insoluble formazan by metabolically active cells. MCF-7 cells were seeded into 96-well plates at a density 1×10^4 cells/well. One day later, the medium was removed and DXR-loaded PLGA nanoparticle suspensions were added to the wells. The cultures were incubated with different concentration DXR-containing PLGA nanoparticles for 24 hours. After incubation, the cultures were washed three times with sterile PBS buffer and returned to incubator for a further 48 hours. Then, the cell medium was changed with 100ul fresh medium and 10µl MTT (5 mg/ ml in sterile PBS buffer) solution. These plates were reincubated for 4hours. The formed formazan crystals were dissolved in DMSO. The absorbance was measured at 540nm using a microplate reader. Cells grown in medium alone were used as a reference as 100% viability. All samples were made in sextuplicates.

3.2.6 Cellular uptake studies by fluorescence microscopy

The cellular uptake of DXR-containing nanoparticles was studied using fluorescence microscopy. Briefly, MCF-7 cells were grown on coverslips for one day to adhere to the surface. The cell cultures were then incubated with DXR-containing nanoparticles at final concentration of DXR at 5 µM for 2 hours. After washed with PBS buffer, the cells were viewed by using a 480/30x bandpass excitation filter, a 505 nm dichroic mirror and a 515nm longpass emission

filter. A slow scan, high performance charged-coupled device (CCD) camera (Andor technology, Model DV 434) with a 1024 × 1024 pixel array was employed to collect digital fluorescence images of the cells.

3.3 Results and Discussion

3.3.1 Characterization of PLGA nanopatricles

The ability of nanometric drug carriers to change the biodistribution and pharmacokinetics of drugs has been found in both vitro and vivo therapeutic applications. Among many factors, particle size and surface properties have been shown to be of primary importance in determining the pharmaceutical characteristics of these drug delivery systems. Administered particles of several micrometers in diameter for example, become entrapped within the lung capillaries. Smaller particles (< 200 nm) are unique in their ability to benefit from EPR effect and avoid spleen-filtering effects [80]. In the present study, PLGA nanoparticles were prepared, using an interfacial polymer deposition (nanoprecipitation) method based on the procedure previous reported by Fessi et al [68]. The PLGA copolymers assembled in aqueous media following precipatation from water-miscible organic solvent. Two different mean size particles (less than 200 nm) were obtained by formulating nanoparticles with different polymer concentration (shown in Table 3.1). TEM analysis revealed that all these particles had a dense, spherical morphology and size distribution is relatively broad (Fig.3.1). A trend of increasing size with the increasing polymer concentration can be observed. The encapsulation efficiency increased

slightly with increasing polymer concentration. However, the encapsulation efficiency was less than 10% in both cases. The low drug loading was due to the hydrophilic nature of Doxorubicin hydrocloride. When drugs were added during the preparation process, they tend to diffuse into aqueous phase.

3.3.2 Fluorescence studies

The inherent fluorescence of DXR was used to characterize the release properties, cellular uptake and intracellular distribution of drug-encapsulated nanoparticles. When excited at 480nm, DXR has fluorescence emission at 590 nm and 560 nm (Fig 3.2a). Fig 3.2b showed the fluorescence image of DXR- loaded PLGA nanoparticles. Clearly, we can see that DXR was entrapped in the nanoaprticles. The fluorescence spectrum of DXR-loaded PLGA nanoparticles was obtained by adding particles into the PBS solution to form the uniform suspension. Fig. 3.3 showed the fluorescence spectra of DXR-loaded PLGA nanoparticles, free DXR and the released DXR from the nanoparticles. The emission spectrum of the released Doxorubicin was similar to that of free Doxorubicin. This indicated that the encapsulation of doxorubicin in PLGA nanoparticles did not affect their structures and spectral properties. The emission of Doxorubicin encapsulated in PLGA nanoparticles showed a change of the ratio between the two characteristic emission peaks of doxorubicin. This could be attributed to the change in the chemical environment of doxorubicin when encapsulated in the particles.

Table 3.1 Nanoparticles formulation and characterization

	Concentration of polymer (mg/mL)	Particle size (nm)	Encapsulation efficiency (%)
a	17	182	8.8 ± 2.1
b	10	110	6.2 ± 1.8

Formulation a

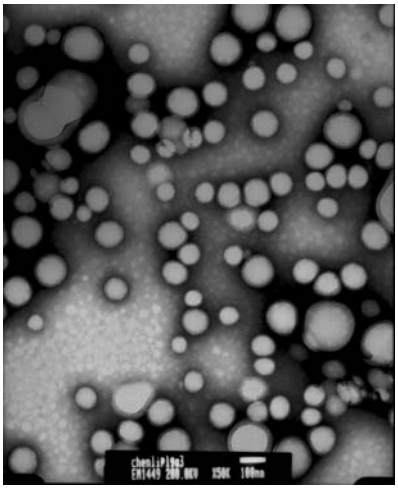

Formulation b

Fig 3.1 Transmission electron images of PLGA nanoparticles (The samples were negatively stained.)

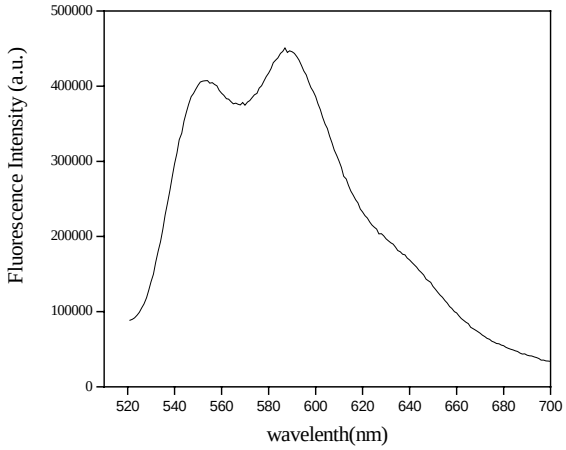

Fig. 3.2 a) Fluorescence emission spectra of DXR in PBS solution

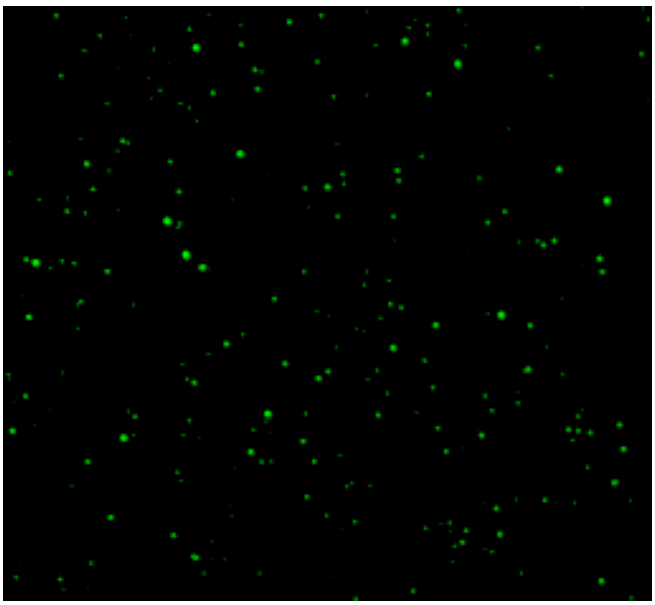

Fig 3.2 b) Fluorescence image of DXR-loaded nanoaprticles .

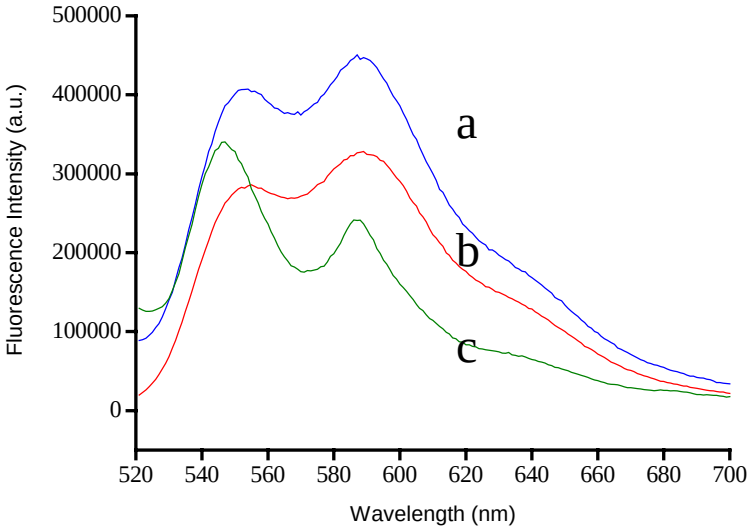

Fig 3.3 Emission spectra of a) Released Doxorubicin from PLGA nanoparticles, b) free Doxorubicin c) Doxorubicin encapsulated in PLGA nanoparticles. (The fluorescence intensities are not comparable since these samples do not have the same concentration.)

3.3.3 In vitro release Studies

The in vitro release profile of DXR was obtained at 37 ^{o}C by representing the percentage of released DXR with respect to the amount of DXR encapsulated in nanoparticles. Fig. 3.4 showed the release profile of DXR loaded nanoparticles that were prepared with different polymer concentrations. The profiles exhibited initial burst release, followed by a slow release in both cases. The release percentage of smaller particles was higher than that of larger particles. But the difference was not significant. Generally, there are mainly two release mechanisms from polymeric nanoparticles: diffusion through the microchannels that were formed during nanoparticles preparation and polymer erosion. In this system, the initial burst release effect is probably dominated by diffusion, rather than polymer erosion.

To examine the effect of pH on the drug release, we also performed the release studies in pH 5 buffer solutions keeping all of other conditions the same. At pH 5, the release rate was slightly enhanced (Fig 3.5). Around 18% and 15% drug content was released in 24 hours at pH 5 and pH 7, respectively. The slight difference in release rate could be attributed to the enhanced solubility of drug at pH 5, since pH have an effect on the drug solubility due to its influence on the ionization of the drug. However, it must be noted that the difference between 18% and 15% in our experiments is too small to come to a clear conclusion. More studies are needed to better understand the effect of pH on drug release properties.

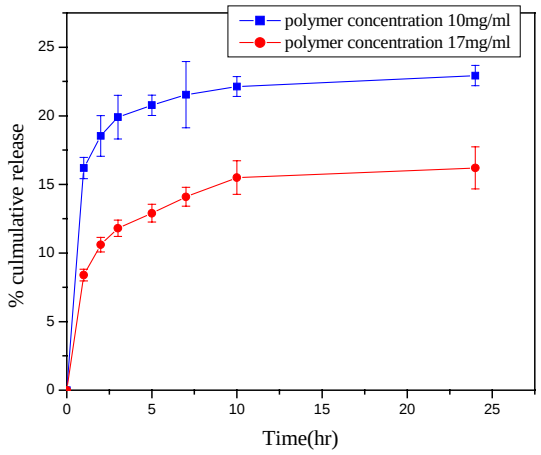

Fig 3.4 In vitro release profile of doxorubicin from PLGA nanoparticles (pH 7.4, 37^{o}C)

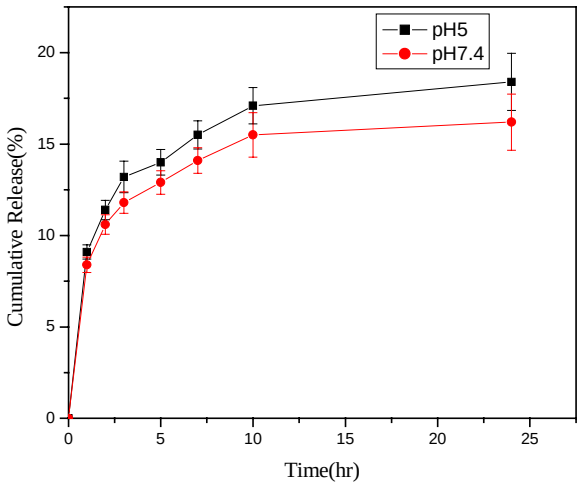

Fig 3.5 Release of Doxorubicin at different pH (polymer concentration 17 mg/ml, 37^{o}C)

3.3.4 Cellular uptake and In vitro cytotoxicity studies

Cellular uptake of DXR-loaded nanoparticles was evidenced by fluorescence microscopy (Fig 3.6). Fig 3.6a is the transmission image of intact cells, which were incubated with free DXR and Fig 3.6 b is the corresponding fluorescence image. Fig 3.6c and 3.6d are the images of cells, which were incubated with DXR-loaded nanoaprticles. These images were taken after 2hours incubation. It is interesting to note here, free DXR was localized within the cell nucleus and DXR-loaded nanoaprticles were localized in the perinuclear region. It could be evidence that DXR-loaded naoparticles were internalized through nonspecific endocytosis due to their small size.

The cytotoxicity of DXR-loaded nanoparticles and free drug were tested against human breast cancer cell line MCF-7 by MTT assay [79]. Blank particles and untreated cell culture were used as control. Fig 3.7 showed cell viability after the cells were exposed to drug-containing nanoparticles with different concentration of DXR for 24 hours at 37^{o}C under 5% CO_2 atmosphere.

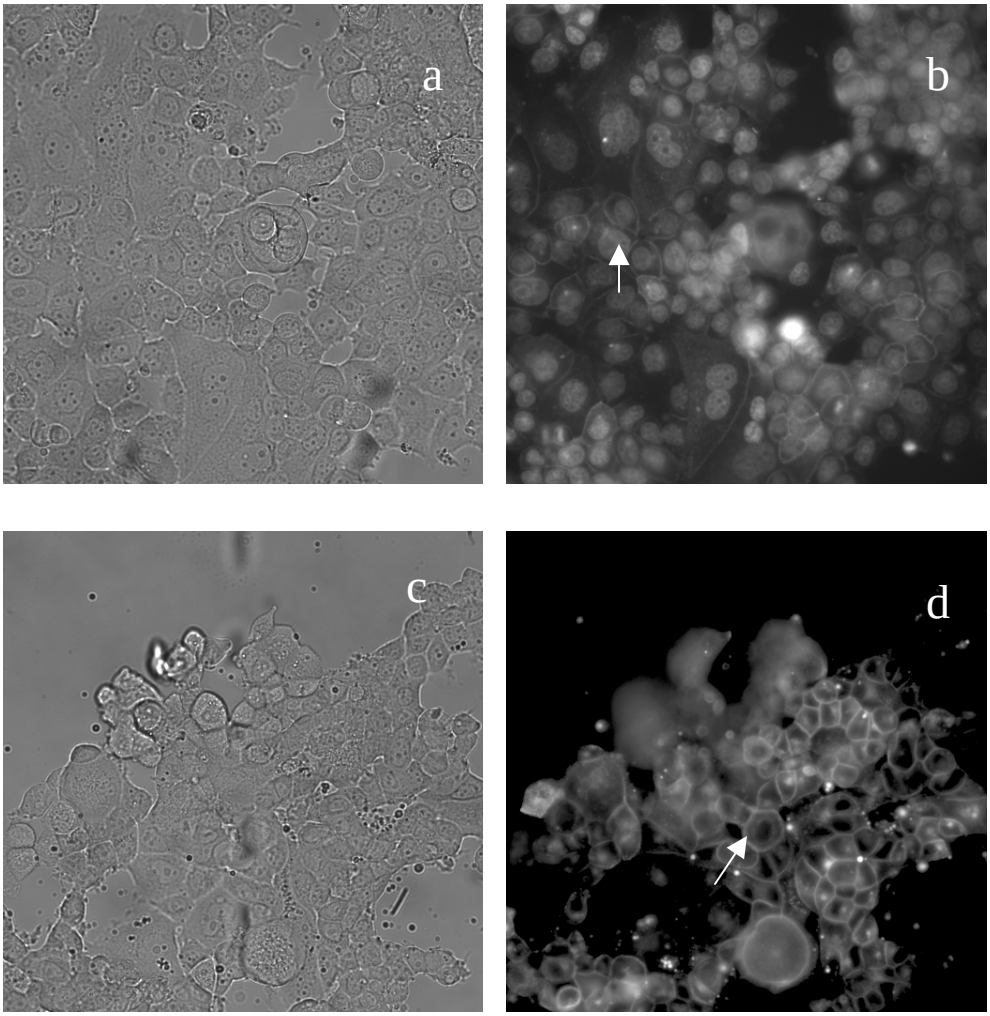

Fig 3.6 Transmission images of MCF-7 cells treated with (a) free DXR (c) DXR-loaded PLGA nanoaprticles. Fluorescence images of (b) free DXR (d) nanoparticles. In image (b), the drugs were localized within the cell nucleus and in image (d) the drugs were localized in the perinuclear region. The cells were incubated with 5μM equivalent DXR concentration. All images were taken with 400x magnification.

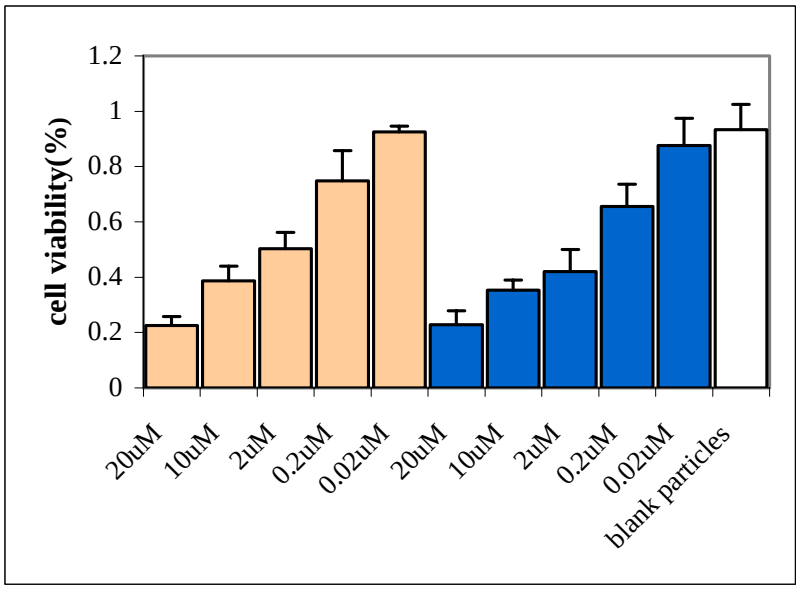

Fig 3.7 The cytocoxicity of DXR-loaded PLGA nanoparticles (mean size 110nm)( ) and free DXR ( ). The density of blank particles is the same as that of drug-load nanoaprticles. Untreated cell cultures were used as a reference as 100% viability.

As we can see in Fig 3.7, no cytotoxicity was observed when the cells were incubated with highest concentration of blank particles. But both drug-loaded nanoparticles and free drug showed concentration dependence cytotoxicity. In both cases, 50% inhibition of cell growth was achieved with around 2μM DXR (IC_{50}). There is no significant difference about drug activity between drug-loaded particles and free drug, which indicated that the cytotoxicity of the drug has been maintained in the nanoparticles.

Numerous studies aimed to develop DXR-loaded colloidal carriers. Some showed enhanced cytotoxicity of drug-loaded carrier compared to free drug [72, 73, 75]. Other studies like ours showed comparable cytotoxicity between drug-loaded carrier and free drugs [74, 76]. R. Tomlinson et al. conjugated DXR with polyacetal and in fact reported decreased cytotoxicity [81]. It seems that cytotoxicity of drug-loaded carrier is mainly affected by the rate of the cellular uptake and the nature of drug carriers, which determine the release properties in cells. Doxorubicin is a DNA-intercalating agent, which targets the cells nucleus. Generally, to travel through the nuclear pore complex, there are two mechanisms depending on molecular size. Small molecules (< 10 nm) can pass across the nuclear envelope by diffusion. Macromolecule and particles (< 25 nm) can only pass through by an energy-dependent process [82]. Therefore, to realize the cytotoxicity of drug-loaded carriers, which is usually larger than 25 nm, drugs must be released from carrier and diffuse into nucleus. The fact that our 110nm nanoparticles maintained drug activity suggested that the nanoparticles first attached and then encapsulated in cellular endosomes. The drugs are then released and diffuse into the cell nucleus. However, Further studies about determining subcellular drug distribution and delivery kinetics in real time have to be conduced to help us to understand the cytocoxicity .

3.4 Summary and Conclusions

This study systematically evaluated the potential of PLGA nanoparticles as drug carriers for anticancer drug Doxorubicin for the first time. Doxorubicin was encapsulated into biodegradable PLGA nanoparticles by simple nanoprecipitation method. The size of particles can be changed by changing the polymer concentration. Fluorescence studies indicated that the encapsulation of doxorubicin in PLGA nanoparticles did not affect their structures and spectral properties. Therefore, we were able to characterize the release properties of system by fluorescence measurements. The release profiles showed that small particles had a higher release rate compared to larger particles. Fluorescence images indicated that these particles can be internalized by human breast cancer MCF-7 cells by non-specific endocytosis. *In vitro* cytotoxicity study showed the drug activity of DXR-containing PLGA nanoparticles has been maintained.

CHAPTER 4 NOVEL SILICA NANOPARTICLES-BASED DRUG DELIVERY SYSTEM TRIGGERED BY ANTIMICROBIAL PEPTIDES

4.1 Introduction

In recent years researchers in the field of drug delivery have attempted to induce drug release from drug carriers using physical or chemical stimuli [10-14]. For the most part the studies involved the use of liposomes [83-86]. Drug release from the liposomes was induced by a change in pH (83), temperature (84), light (85) and magnetic field (86). Polymer nanoparticles were recently developed as alternative drug carriers to replace liposomes since liposomes often show limited capability as drug carriers (87). Efficient drug loading into liposomes has proved difficult. Additionally, drug molecules tend to leak out of liposomes prior to their localization in a targeted tissue. This decreases the therapeutic efficiency and causes undesirable side effects.

Recently, several groups explored the use of porous silica nanoparticles as drug delivery carriers [63-66]. Although silica particles are not biodegradable, the potential advantages of porous silica nanoparticles as drug carriers cannot be ignored. First, it has been shown that silica nanoparticles are biocompatible [61]. Second, porous silica materials have a large surface area and therefore effectively host large amounts of drug molecules. Furthermore, the pore size and

surface properties of mesoporous silica particles are easily controlled by changing conditions during their synthesis [88, 89]. Recent studies demonstrated that drug and protein molecules could be encapsulated with high loading efficiency in porous silica nanoparticles [63, 65, 90]. However, while the loading efficiency was indeed high the leakage rate of the encapsulated molecules was high as well. A mechanism to minimize leakage of encapsulated molecules from porous silica particles and trigger the release by a chemical or physical stimulation is needed to facilitate their use as drug carriers.

In a recent study Lin and coworkers addressed the issue of minimizing leakage and triggered release from porous silica nanoparticles [66]. Following the encapsulation of ATP molecules in porous silica nanoparticles the pores of the particles were blocked by the covalent attachment of CdS nanocrystals to the surface of the particles. This effectively blocked leakage of ATP from the particles. ATP release was then triggered by incubating the CdS capped silica particles in a solution that contained reducing agents like dithiothreitol and mercaptoethanol. Lin and coworkers showed that the CdS nanocrystals-coated silica nanoparticles did not affect the growth of astrocytes. However, it is reasonable to expect that CdS nanocrstals would not be ideal plugs to contain drug molecules in porous silica particles. Furthermore, the use of high levels of reducing agents to induce drug release *in vivo* may not be a viable option due to expected cytoxicity of the reducing agents themselves. In this chapter we describe the use of a phospholipid membrane to block the release of drug molecules from porous silica nanoparticles (Fig. 4.1) and a new triggering mechanism, based on the use of low levels of antimicrobial peptides to induce drug release from these particles. The advantages and limitations of this new-triggered release technology are discussed.

4.2 Specific Experimental and Technical Details

4.2.1 Characterization of silica nanoparticles

The morphology and size of particles were characterized using Transmission electron microscopy (TEM). Specimens were prepared by dispersing the as-obtained powder in alcohol and then placing a drop of suspension on a copper grid coated with transparent graphite, followed by drying. Particles size and size distribution were analyzed by image ProPlus from TEM images taken from different fields.

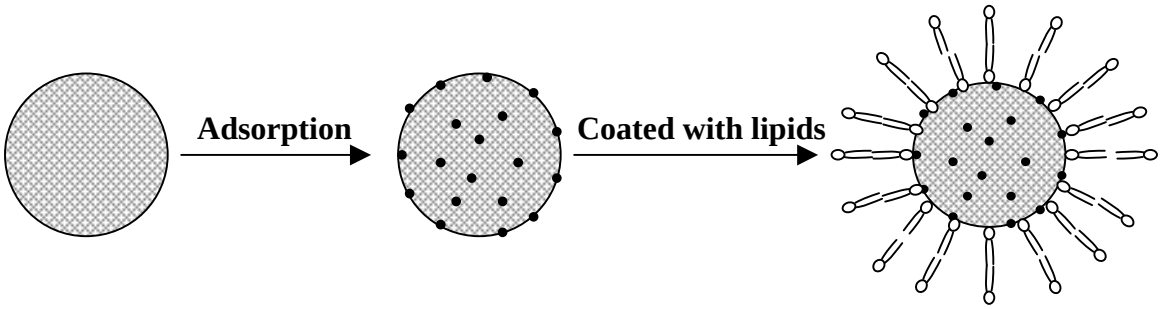

Fig. 4.1. Schematic representation of formation of phospholipid coated mesoporous silica nanoparticles as drug carriers.

4.2.2 Studies of TMR-Dex release profiles

The *in vitro* release studies of TMR-Dex from nanoparticles were carried out in 10 mM HEPES buffer solution. 17.5mg TMR-Dex loaded silica lipobeads were dispersed in 10mL buffer. The solution was sonicated for minute to obtain monodispersity. Then the suspension was divided into 1 ml ×10 aliquots. At various time intervals, 1 ml suspension was taken and the free TMR-Dex was washed by centrifugation for 5 min at 12000 rpm. The particles were then resuspended in 1 mL buffer solution and the fluorescence spectrum of the suspension was recorded using the fluorimeter. The retained percentage of TMR-Dex at various times was calculated by comparing the fluorescence intensity of the suspension at t = t' and t= 0, where t' represents aspecific time interval. Samples were kept in the dark all the time. All samples were made in triplicates to enable quantitative data analysis.

To study the effect of temperature, the release was carried out in HEPES buffer solution at pH 7.4 at room temperature and 42^{o}C.

4.2.3 The effects of antimicrobial peptide cecropin-melittin

The dependence of the %-released contents on peptide concentration was determined in 10 mM HEPES buffer solution at pH 7.4. Different amounts of cecropin-melittin were added to 500 µL TMR-DEX loaded silica lipobeads. Then, the total volume was brought to 1mL by adding HEPES buffer solution. After 2hours, the free dye was removed by centrifugation and the

particles were resuspended in 1mL fresh HEPES buffer. The percentage of retained dye was calculated as described above.

4.3 Results and Discussion

4.3.1 Synthesis of mesoporous silica nanoparticles

Silica nanoparticles are attractive candidates for many applications such as chemical sensing, ion-exchange coating and chromatography [91]. Extensive studies were carried out using silica materials which were prepared by the sol-gel process. In a typical sol-gel process, tetraalkylsilane is mixed with water followed by the addition of catalyst. Tetraalkylsilane can be hydrolyzed and condensed to form the sol and the sol is further crosslinked through polycondensation to form a rigid, porous network-gel. However, the limitation of sol-gel materials is their variability in pore size, which cannot be tailored for specific molecules. Discovery of mesoporous silica materials made it possible to tailor both pore size and structure of these materials for specific hosts. Mesoporous silica materials are synthesized by self-assembly of silica-surfactant in which inorganic species simultaneously condense, giving rise to mesoscopiclly ordered composites formation [69, 92]. Well-defined pore size depends mainly on the surfactant, which is employed as a template in the synthesis. In our study, mesoprous silica nanoparticles were synthesized using a method developed by Cai [69]. TEM images revealed that the average size of nanoparticles was around 90 nm with narrow size distribution. The particles exhibited elongated sphere morphology (Fig 4.2).

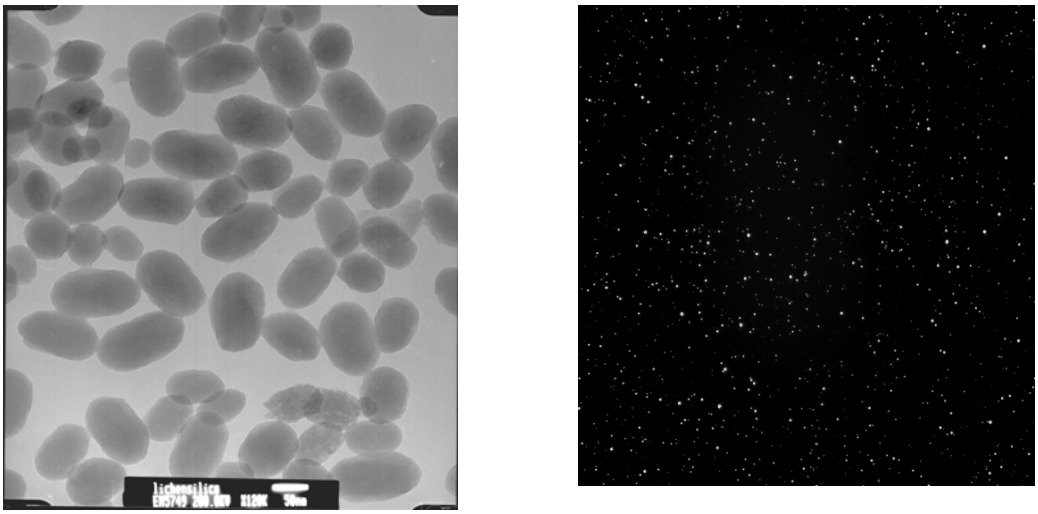

Fig. 4.2 (A) TEM (B) Fluorescence images of TMR-DEX loaded silica nanoparticles. The average size of the nanoparticles was around 90 nm.

4.3.2 Loading studies of TMR-Dex into silica nanoparticles

To easily monitor the drug- loading and release properties of the particles, we chose the fluorescent dye-tetramethylrhodamine dextran (3000Da)(TMR-Dex), which has high extinction coefficient, stability and pH insensitivity, as a drug analog. To load the dye into the particles, mesoporous silica nanoparticles were dispersed in TMR-Dex solution at pH 3 for 24 hours. Electrostatic attraction between the protonated TMR-Dex due to the acidic conditions and the negatively charged silica enhanced the entrapment efficiency of TMR-Dex in the silica particles. The dye content in the particles was measured by monitoring the difference in the fluorescence of the preparation solution prior and following dye entrapment into the particles. The loading efficiency was about 28±2%. However, TMR-Dex molecules diffused out of the particles under physiological pH conditions due to decreasing electrostatic attraction forces.

4.3.3 Lipids membrane coating of TMR-DEX-loaded silica nanoparticles

Liposomes were extensively studied for drug delivery and chemical sensing. They have a flexible, cell-like lipid bilayer surface, which acts as a permeability barrier such that compounds can be entrapped in their aqueous interior. However, liposomes can be mechanically unstable and their loading capacity is relatively low compared to solid particles. Previously, lipid bilayers supported on various solid surfaces, such as glass [93], plastic [94], and metal [95] as well as modified polymers [96] have been shown to provide a stable and well-defined cell-membrane-like environment. Based on this knowledge, several groups proposed hybrid vesicle systems, which have polymer nanoparticles as core and lipid bilayer as shell [97-100], termed lipobeads. In our group, lipobeads were used for intracellular sensing [99,100]. Our studies showed that the phospholipid membrane protected sensing elements from cellular environment.

The objective of our study was to realize stable drug containing nanoparticles that only release their content instantly when stimulated. To this end the particles were coated with a phospholipids membrane using a procedure previously developed in our laboratory for the fabrication of lipobead-based nanosensors. The silica lipobeads were washed several times to remove dye molecules that leaked out of the particles prior to applying the phospholipid membrane and re-adsorbed to the membrane following the formation of the membranal coating. Temporal release profiles shown in figure 4.3 indicate that the phospholipids membrane efficiently blocked leakage of dye molecules from the silica lipobeads. Almost 95% of the TMR-Dex retained in phospolipid coated silica nanoparticles over 12 hours. In contrast, about

90% of the TMR-Dex molecules leaked from uncoated silica matrix in 12 hours following their preparation.

To examine the effect of temperature, the release experiment also carried out at 42 ^{o}C with silica DMPC-lipobeads. We expected an increased release since DMPC had a phase transition at 24 ^{o}C [101]. Above the phase transition temperature, lipid bilayers undergo a change in structure, switching from a gel state where acyl chains of the lipids molecules are closely organized, to a sol state where the acyl chins are disorganized. Therefore, the lipid bilayer is more fluid. Surprisingly, the release was the same as that of room temperature within 4 hours (Fig. 4.4). After this time, the release increased rapidly. The possible reason is that the TMR-Dex molecule were too large to pass through bilayer membrane even at sol state. But overheating (longer than 4 hours) could destabilize the lipid membrane. The same experiments were carried out when the particles were coated with DPPC lipid. Similar results were observed.

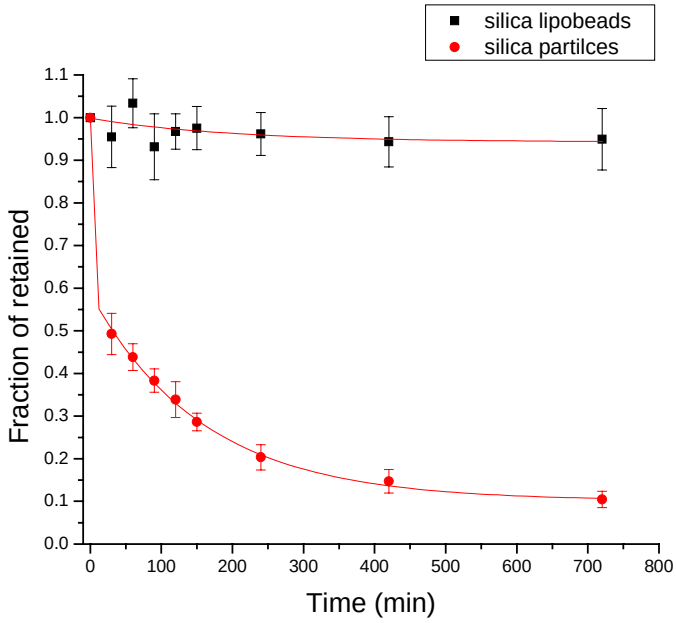

Fig. 4.3 Release profile of TMR-Dex loaded silica particles in 10mM HEPES pH7.4 buffer solution.

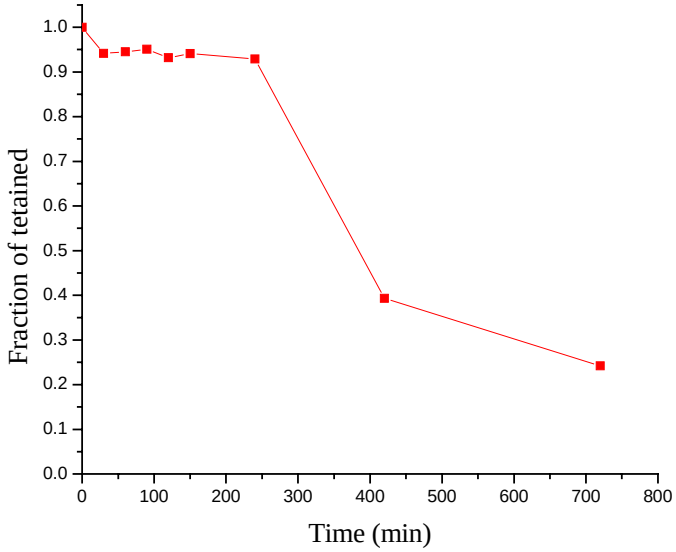

Fig. 4.4 Release profile of TMR-Dex loaded silica DMPC-lipobeads in 10mM HEPES pH7.4 buffer solution at 42^{o}C.

4.3.4 The induced release of TMR-DEX by antimicrobial peptide

As mentioned previously, the development of drug carriers that effectively encapsulate the drug with minimal leakage and only release it when triggered chemically or physically would be highly beneficial to many clinical situations. The selection of an appropriate triggering strategy is crucial. For example, pH- sensitive drug carriers would release their content as a result of a pH change in a tissue. In many cases the pH required for effective release is unreachable. Similarly, drug carriers that rely on temperature changes to induce release are limited because of the narrow temperature range under physiological conditions and the relatively wide range of body temperature of normal patients. In this study we explored the use of low concentrations of antimicrobial peptides to induce the release of our fluorescent drug analog TMR-Dex from the silica lipobeads. Antimicrobial peptides are a group of small peptides that show a broad range of activity against Gram-negative and Gram-positive bacteria, fungi, mycobacteria and some enveloped viruses [102]. These peptides attracted increasing attention in recent years since they represent a promising new alternative for conventional antibiotic drugs. These peptides could provide a solution to the growing problem of antibiotic resistance [102]. The mechanism of action of these peptides involves increasing cell membrane permeability either by forming aqueous channels which span the membrane bilayer or by disrupting membrane organization [102,103]. We predicted that antimicrobial peptides could disrupt the membranal coating of the silica lipobeads to facilitate the release of TMR-Dex from the particles. To test this triggered release strategy, our TMR-Dex containing lipobeads were incubated with solutions of the antimicrobial peptide- Cecropin A(1-8)-Melittin(1-18) hybrid. The phospholipids membrane of the silica lipobeads was composed of 1,2-Dimyristoyl-sn-

Glycero-3-Phosphocholine (DMPC). Temporal release profiles of TMR-Dex silica lipobeads upon addition of antimicrobial peptide are shown in figure 4.5. Curve a shows a control experiment in the absence of the peptides in which no release is seen, indicating that the membrane remained intact throughout the experiment. Curves b shows that the release was rapidly triggered after the addition of 0.175 mg/mL Cecropin A-Melittin. About 70% of dye contents were released. Also, the dependence of the %-released contents on peptide concentration was studied. As Fig. 5 showed, a maximum release was obtained at 0.350mg/mL peptides and minimum peptide concentration 0.044mg/mL was required to induce the release effectively.

The effect of Cecropin A(1-8)-Melittin(1-18) hybrid on the negatively charged phospholipids Bovine brain phosphatidylserine (PS) coated silica particles was also tested. As Fig.4.6 and 4.7 showed, the cecropin A-melittin is more effective on the negatively charged PS lipobeads than on the neutral DMPC lipobeads. This may result from the cationic nature of the peptide at pH 7. Further studies about dependence of the %-released contents of PS lipobeads on peptide concentration are in progress.

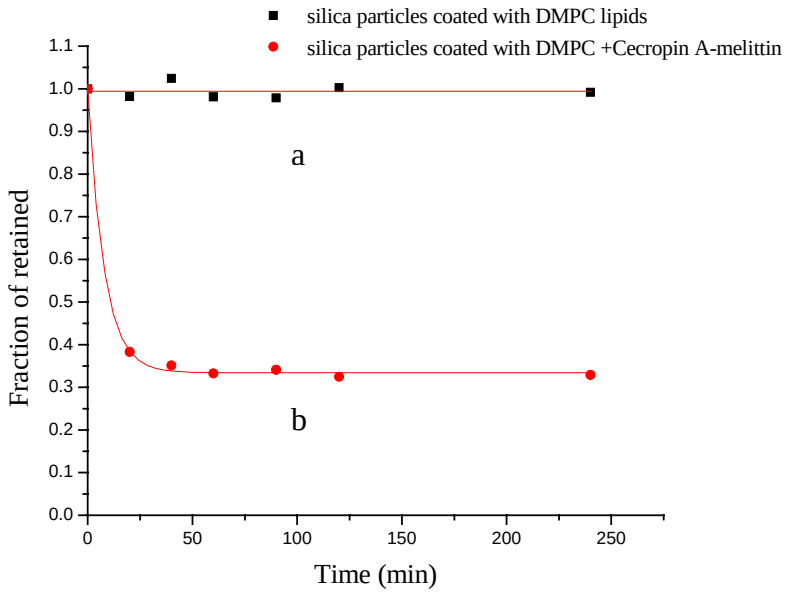

Fig. 4.5 Release profiles of silica DMPC-lipobeads treated with 0.175 mg/mL Cecropin A-melittin peptide.

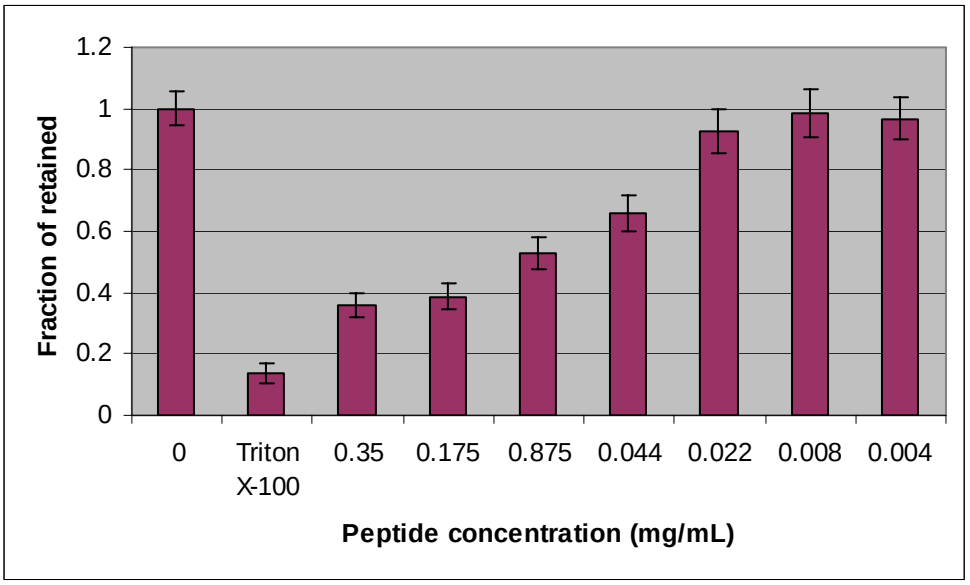

Fig. 4.6 Peptide concentration-dependent release. (The measurements were taken 2 hours after addition of cecropin-melittin peptide).

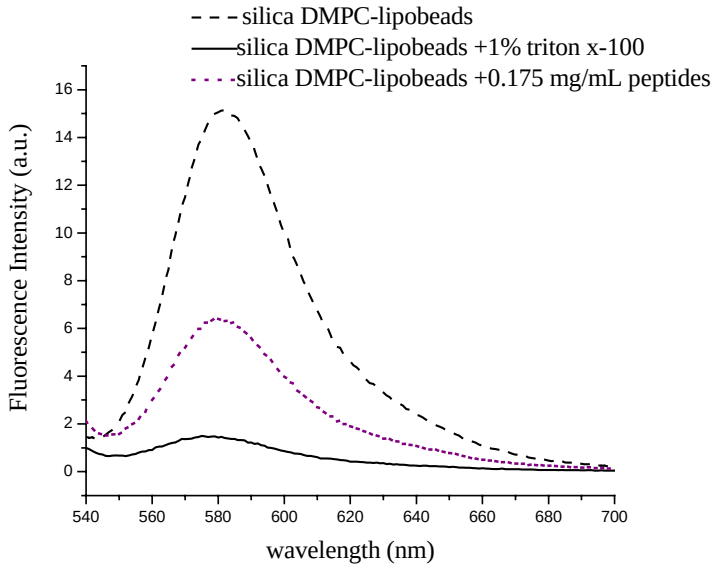

Fig. 4.7 Fluorescence spectra of silica DMPC-lipobeads (Measurements were taken 2 hours after peptides were added)

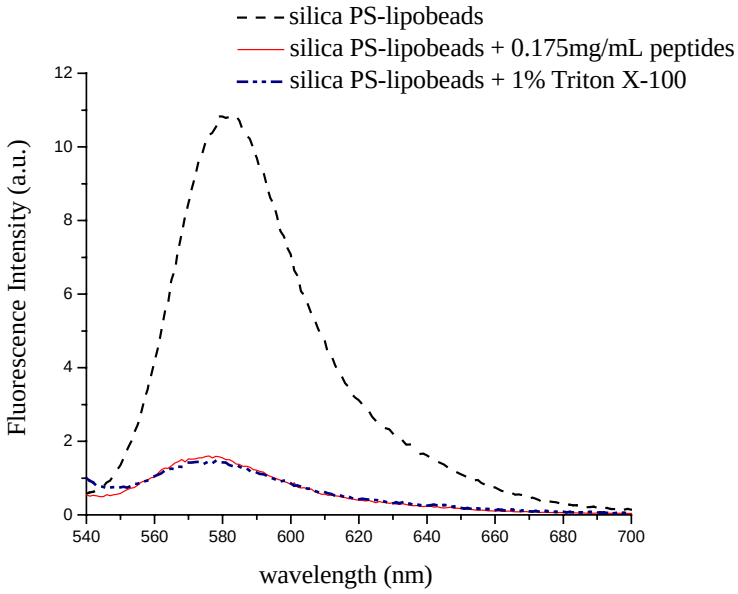

Fig. 4.8 Fluorescence spectra of silica PS-lipobeads (Measurements were taken 2 hours after peptides were added)

4.4 Summary and Conclusions

In summary, we have developed a novel silica nanoparticles-based drug delivery system, which enables high drug loading and regulated drug release by adjusting the level of an adjuvant drug. While this approach show clear advantages over physical stimulation like temperature change or other non-selective and unregulated pH changes the toxicity of antimicrobial peptides still remained a concern. Future work is in progress to seek a lipid membrane which would be selectively destroyed by peptides that do not harm living cells.

CHAPTER 5 SUMMARY AND CONCLUSIONS

Controlled drug delivery can influence the performance of a drug by manipulating its concentration, location and duration. Therefore, it provides a promising way to minimize side effects and increase therapeutic efficacy. In the past decades, controlled drug delivery technology has represented one of the frontier areas of science, which involves multidisciplinary scientific approach. This thesis describes the development and characterization of new nanoparticles-based drug carriers with unique release properties.

Chapter 3 describes the development of a polymeric nanoparticle-based drug delivery system for the anticancer drug doxorubicin. Biodegradable poly (lactide-co-glycolide) (PLGA) particles of various sizes were prepared by changing the polymer concentration. Transmission electron microscopy (TEM) images revealed that the particles had smooth spherical morphology with a mean size ranging from 110nm to 180nm. The *in vitro* release profile showed that small particles (110nm) had a higher release rate compared to larger particles (180nm). For all nanoparticles prepared with different polymer concentration, an initial burst release, followed by a slow release, were observed. These results indicated that the drugs were released through a diffusion-controlled release mechanism. Fluorescence imaging studies showed that the nanoparticles could be internalized by MCF-7 human breast cancer cells. Interestingly, different intracellular distribution of free drugs and the drug-loaded nanoaprticles were observed. It

indicated that they were taken up by different mechanism. Probably free drugs were taken up by diffusion and nanoparticles were internalized by non-specific endocytosis. The bioactivity of the drugs was also tested against MCF-7 cell culture. *In vitro* cytotoxicity study showed that drug activity had been maintained in these particles.

In Chapter 4, we reported the preparation of mesoporous silica nanoparticles and their use in triggered drug release system. Silica nanoparticles, which can be prepared with a desired size, tunable pore size and surface properties, were previously used as hosts of proteins and catalysts. We loaded the mesoporous silica nanopartilces with the tetramethylrhodamine dextran (TMR-Dex), which was used as a fluorescent drug analog. We then coated the nanoparticles with a phospholipid membrane to seal drug molecules inside the nanoparticles. Temporal release profiles showed that 95% of the TMR-Dex molecules were retained in phospholipids coated silica nanoparticles over 12 hours. In contrast about 90%of the TMR-Dex molecules leaked from uncoated silica particles during the same time period. The release of TMR-Dex molecules from phospholipids coated silica particles was triggered by adding the antimicrobial peptide cecropin-melittin to the particle suspension. About 70% of TMR-Dex molecules were released in 2 hours following the addition of 0.175mg/mL cecropin-melittin (final concentration). The regulated release of the encapsulated content was realized by adjusting the level of the antiimicrobial peptide cecropin (1-8)-melittin (1-18). Further studies will focus on optimizing the composition of lipids membrane to selectively destroy the coating without inducing toxicity to living cells.

References

1. Lee, K.Y.; Peters, M. C.; Mooney, D. J. *Adv. Mater*., **2001**, 13, 837- 839
2. Lasic, D. D. *Polymer news*, **1998,** 23, 367-375
3. Brannon-peppas, L.; Birnbaum, D.T.; Kosmala, J. D. *Polymer news*, **1997**, 22, 316-318
4. Uhrich, K. E.; Cannizaaro, S. M.; Langer, R. S. *Chem. Rev*., **1999**, 99, 3181-3198
5. Langer, R. S. *Nature*, **1998**, 392-395
6. Panyam, J.; Labhasetwar, V.; *Adv. Drug Deliv. Rev*., **2003**, 55, 329-347
7. Muller, R. H.; Radtke, M.; Wissing, S. A. *Adv. Drug Deliv. Rev*., **2002,** 54 suppl. 1, S131-S155
8. Perez, C.; Sanchez, A.; Putnam, D.; Ting, D.; Langer, R.; Alonso, M. J. *J. Controlled Release*, **2001**, 75, 211-224
9. Kumar, N.; Ravikkumar, M.; Domb, A. J. *Adv. Drug Deliv. Rev*., **2001**, 53, 23-44
10. Mikashi, T.; Asami, N.; Uragami, T. *Nature*, **1999**, 399, 766-769
11. Lee, K.; Peters, M. C.; Mooney, D. J. *Adv. Mater*., **2001**, 13, 837-839
12. Kohane, D. S.; Anderson, D. G.; Yu, C.; Langer, R. *Pharml. Res.*, **2003**, 20, 1533-1538
13. Kono, K. *Adv. Drug Deliv. Rev*., **2001**, 53, 307-319
14. Kost, J.; Langer, R. *Adv. Drug Deliv. Rev*., **2001**, 46, 125-148
15. Illum, L.; Davis, S. S.; Wilson, C.G.; Frier, M.; Hardy, J. G.; Thomas, N. W. *Int. J. Pharm.*, **1982**, 12, 135-146
16. Illum, L.; Davis, S. S. *FEBS letter*., **1984**, 167, 79-82
17. Desai, A.G.; Thakur, M.L.; *Semin. Nucl. Med.*, **1985**, 3, 229-239
18. Diepold, R.; Kreuter, J.; Guggerenbuhl, P.; Robinsin, J. R. *Int. J. Pharm*, **1989**, 54, 149-153
19. Duncan, T.A.; Connors, H. *J. Drug Targeting*, **1996**, 3, 317-319
20. Monsky, W.L.; Fukumura, D.; Gohongi, T. *Cancer Res*., **1999**, 59, 4129-4135
21. Li, H.; Qian, Z. *Med. Res. Rev*., **2002**, 22, 225-250
22. Reddy, J. A.; Low, P.S. *Crit. Rev. Ther. Drug Carrier Syst.*, **1998**, 15, 587-627
23. Tomlinson, E.; Burger, J. J. *Polymers in controlled Drug delivery*, Wright, Brostol, **1987**, pp25-48
24. Chen, J.; Gamou, S.; Takayanagi, A.; Ohtake,Y.;Ohtsubo, M.; Shimizu, N. Hum. *Gene Ther.*, **1998**, 9, 2673-2681
25. Bangham, A.D.; Standish, M.M.; Watkins, J.C. *J. Mol. Biol.*, **1965**, 13, 238-252
26. Crommelin, D.J.A.; Schreier, H.; Liposomes. In: Colloidal Drug Delivery System; Marcel Dekker, New York, 1994,73-98
27. Gregoriadis, G. *Trends Biotech*., **1995**, 13, 527-541
28. Gregoriadis, G.; Florence, A. T. *Drugs*, **1993**, 45, 15-28
29. Lasic, D.D. *Nature*, **1996**, 380, 5611-5620
30. Gerasimov, O.V.; Boomer, J. A.; Qualls, M. M. *Adv. Drug Deliv. Rev*., **1999,** 317-338

31. Kaneda, Y.; *Adv. Drug Deliv. Rev*., **2000**, 43, 197-205
32. Lim, H. J.; Masin, T.D.; Madden, M.B.; Bally, M. B. *J. Pharm. Exp. Therapeut.,* **1997**, 281, 566-573
33. Cullis, P. R.; Hope, M.J.; Bally, M.B.; Madden, T. D.; Mayer, L. D.; Fenske, D.B. *Biochim. Biophys. Acta*., **1997**, 1331, 187-211
34. Bakker-Woudenberg, J. M.; Tenkate, M.T.; Stearne-cullen, L. E .T.; Woodle, M.C. *J. Infect. Disease*, **1995**, 17, 938-947
35. Babincova, M; Sourivong, P.; Chorvat, D.; Babinec, P. *J. Magnetism and Magnetic Mater.*, **1999**, 194, 163-166
36. Babincova, M; Sourivong, P.; Chorvat, D.; Babinec, P. *Bioelectrochemistry*, **2002**, 55, 17-19
37. Chen, H.; Langer, R. *Pharm. Res*., **1997**, 14, 537-540
38. Zhigaltsev, I. V.; Maurer, N; Wong, K. F. and Cullis, P.R. *Biochim. Biophys. Acta.*, **2002**, 1565, 129-135
39. Chu, C.; Szoka, F. *J. Liposome Res.*, **1994**, 4, 361-395
40. Chonn, A.; Cullis, P.R. *Curr. Opin.Biotech*, **1995**, 6, 698-708
41. Forseen, E. A.; Male-Brune, R.; Adler-Moore, J. P.; lee, M. J. A.; Schmit,P.G *Cancer Res.*, **1996**, 56, 2066-2075
42. Scherphof, G. L.; VanBorssum, M. *J. Liposome Res.*, **1994**, 4, 427-437
43. Boman, N.L.; Masin, D.; Mayer, L. D.; Cullis, P. R.; Bally, M. B. *Cancer Res.*, **1994**, 54, 2830-2833
44. Allen, T. M.; Newman, M. S.; Woodle, M. C.; Mayhew, E. *Int. J. Can.*, **1995**, 62, 199-204
45. Mayer, L. D.; Masin, D.; Nayar, R.; Boman, N. L; Bally, M. B. *Br. J. Cancer*, **1995,** 71, 482-488
46. Tari, A. M.; Tucker, S.D.; Deisseroth, A.; Lopez-Berestin, G. *Blood,* **1994**, 84, 601-607
47. Tari, A. M.; Andreeff, M.; Kleine, H. D.; Lopez-Berestin, G. *J. Mol. Med.*, **1996**, 74, 623-628
48. Yokoyama, M. *Crit. Rev. Drug Carr. Sys.*, **1992**, 9, 213-248
49. Chari, R. V. J. *Adv. Drug Deliv. Rev*., **1998**, 31, 89-104
50. Caliceti, P.; Salmaso, S.; Semenzato, A.; Carofiglio, T.; Fornasier, R.; Fermeglia, M. *Bioconjugate Chem.,* **2003**, 14, 899-908
51. Kopeccek, J.; Duncan, R. *J. Controlled Release*, **1987**,6, 315
52. Hershfield M. S.; Buckley, R. H. *N. Engl. J. Med.*, **1987**, 316, 589
53. Chen, H.; Neerman, M.; Parrish, A.R.; Simanek, E. E. *J. Am. Chem. Soc.,* **2004**, 126, 10044-10048
54. Sakuma, S.; Hayashi, M.; Akashi, M. *Adv. Drug Deliv. Rev*., **2001**, 47, 21-37
55. Brigger, I.; Dubernet, C.; Couvreur, P. *Adv. Drug Deliv. Rev*., **2002,** 54, 631-651
56. Matsusue, Y.; Hanafusa, S.; Yamamuro, T.; Shikinami,Y.; Ikada, Y. *Clin. Orthop*. , **1995**, 317, 246-253
57. Calvo, P.; Remunan-Lopez, C.; Vila-Jato, J. L.; Alonso, M. J. *Pharm. Res.*, **1997**, 14, 1431-1436
58. Mladenovska, K.; Kumbaradzi, E.F.; Dodov, G. M.; Makraduli, L.; Goracinova, K. *Int. J. Pharm*., **2002**, 242, 247-249
59. Fernandez-urrusuno, R.; Calvo, P,; Remunan-Lopez, C.; Vila-Jato, J. L.; Alonso, M. *J. Pharm. Res.*, **1999**, 16, 1576-1591
60. Edwards, D. A.; Hanes, J.; Caponetti, G.; Hrkach, J.; Ben-Jebria, A.; Eskew, M.L.; Mintzes, J.; Deaver, D.; Lotan, N.; Langer, R. *Science*, **1997**, 276, 1868-1871

61. Jain, T. K.; Roy, I.; Maitra, A. N. *J. Am. Chem. Soc.*, **1998**,120,11092-11095
62. Roy, I.; Ohulchanskyy, T. Y.; pudaver, H. E.; Bergey. E.; Oseroff, A. R.; Morgan, J.; Dougherty, T. J.; Prasad, P. N. *J. Am. Chem. Soc*., **2003**, 125, 7860-7865
63. Han, Y.; Stucky, G. D.; Butler, A. *J. Am. Chem. Soc*., **1999**, 121, 9897-9898
64. Muñoz, B.; Rámlia, A.; Pérez-Pariente, J.; Díaz, I.; Vallet-Regí, M. *Chem. Mater.*, **2003**, 15, 500-503
65.Vallet-Regí, M.; Rámlia, A.; del Real, R.P.; Pérez-Pariente, J. *Chem. Mater*. **2001**, 13, 308-311
66. Lai, C.; Trewyn, B. G.; Jeftinijia, D. M.; Jeftinijia, K.; Xu, S.; Jeftinijia, S.; Lin, V. *J. Am. Chem. Soc.*, **2003**, 125, 4451-4459
67. Savic, R.; Luo, L.; Eisenberg, A.; Maysinger, D. *Science*, **2003**, 300, 615-618
68. Fessi, H; Puisieux, F.; Devissaguet, J.P.; Ammoury, N.; Benita, S. *Int. J. Pharm.*, **1989**, 55, R1-R4
69. Cai, Q.; Luo, Z.; Pang, W.; Fan, Y.; Chen, X.; Cui, F. *Chem. Mater.*, **2001,** 13, 258-263
70. Booser, D.J.; Hortobagyi, G. N. *Drugs,* **1994**, 47, 223
71. Myers, C.E.; Chabner, B.A. *Cancer Chemotherapy*, Lippincott, Philadelphia, **1990**, pp.356-381
72. Gokhale, P.C.; Radhakrishnan, B.; Rahman, A. et al, *Br. J. Cancer*, **1996**, 34, 45-48
73. Nakanishi, T.; Fukuchima, S.; Okamoto, K. et al *J. controlled Release*, **2001**, 74, 295-302
74. Lee, E.; Na, K.; Bae, Y. *J. Controlled Release***, 2003**, 91, 103-113
75. Miglietta, A.; cavalli, R.; Gasco, M.R. et al *Int. J. Pharm*., **2000,** 61-67
76. Janes, K.; Fresneau, M.; Alonso, M. *J. Controlled Release*, **2001**, 73, 255-267
77. Astier, A.; Doat, B.; Ferrer, M. *Cancer Res.*, **1988,** 48, 1835-1841
78. Yoo, H.; Oh, J.; Lee, K.; Park, T. *Pharma. Res.*, **1999**, 16, 1114-1118
79. Hansen, M.B.; Nielsen, S.E.; Berg, K. *J. Immun. Methods*, **1989**, 119, 203-210
80. Mohimi, S.M.; Porter, C.J.H.; Muir, I. S.; Illum, L.; Davis, S.S. *Biochem. Biophys. Res. Commun.*, **1991**, 177, 861
81. Tomlinson, R.; Heller, J.; Brocchini, S.; Duncan, R. *Biocounjate Chem.*, **2003**, 14, 1096-1106
82. Cooper, G. E. *The cell: A Molecular Approach*, ASM press, Sunderland, Massachusetts, pp.319-320
83. Shin, J.; Shum, P.; Thompson, D.H. *Journal of Controlled Release*, **2003,** 91, 187-200
84.Weinstein, J.N.; Magin, R.L.; Yatvin, M.B.; Zaharko, D. S. *Science*, **1979**, 204, 188-191
85. Morgan, C. G.; Thomas, E. W.; Yianni, Y.P.; Sandhu, S. S. *Biochim. Biophys. Acta*, **1985**, 820, 107-114
86. Babincova, M.; Altanerova, P.; Altaner, C.; Babinec, P. Bioelectrochemistry, **2002**, 55, 17-19
87. Woodle, M. C.; Lasic, D. D. *Biochim. Biophys. Acta*, **1992**, 1113, 171-199
88. Kresge, C. T.; Leonowicz, M. E.; Roth, W.J.; Vartuli, J. C.; Beck, J. S. *Nature,* **1992**, 359, 710
89. Zhao, D.; Feng, J.; Huo, Q.; Melosh, N.; Fredrickson, G. H.; Chmelka, B.F.; Stucky, G. D. *Science*, **1998**, 279, 548
90. Wang, Y.; Caruso, F. *Chem. Commun.* **2004**,1528-1529
91. Collinson, M. M. *Trends in Anal. Chem*., **2002**, 21, 30-38
92. Nooney, R.I.; Thirunavukkarasu, D.; Chen, Y.; Josephs, R.; Ostafin, A. Chem. Mater., **2002**, 14, 4721-4728

93. Bayer, T. M.; Bloom, M. *Biophys. J.*, **1990**, 58, 357-362
94. Rothe, U.; Aurich, H.; Engelhard, H.; Oesterhelt, D. *FEBS Lett.*, **1990**, 263, 308-312
95. Plant, A. L. *Langmuir*, **1993**, 9, 2764-2767
96. Spinke, J.; Yang, J.; Wolf, H.; Liley, M.; Ringsdorf, H.; Knoll, W. *Biophys. J.*, **1992,** 63, 1667-362
97. Major, M.; Prieur, E.; Tocanne, J. F.; Betbeder, D.; Sautereau, A.M. *Biochim. Biophy. Acta.*, **1997**, 1327, 32-40
98. Jin, T.; Pennefather, P.; Lee, P. I. *FEBS Lett.*, **1996,** 397, 70-74
99. Jin, J.; Rosenzweig, N.; Jones, I.; Rosenzweig, Z. *Anal. Chem.*, **2001**, 73, 3521-3527
100. Kerry, P. M.; Nguyen, T.; Dumitrascu, G.; Jin, J.; Rosenzweig, N.; Rosenzweig, Z. *Anal.Chem.*, **2001**, 73, 3240-3246
101. Ortiz, A.; Aranda, F. J.; Gomez-Fernandez, J. C. *Biochim. Biophys. Acta***., 1987**, *898*, 214.
102. Zasloff, M. *Nature*, **2002**, 415,389-395
103. Shai, Y. *Biochim. Biophys. Acta*, **1999**, 1462, 55-70

VITA

The author was born in Henan, China. In 1989, she began her undergraduate study in Zhengzhou University, where she obtained her B.S. degree in Chemistry Department in 1993. She continued her graduate study in organic chemistry at Lanzhou Institute of Chemical Physics, Chinese Academy of Sciences and earned a M.S. degree in 1996. In 2000, she joined the Department of Chemistry at the University of New Orleans and became a member of Professor Zeev Rosenzweig's research group.